Therapeutics, Targets, and Chemical Biology

Cancer Research

Tumor Detection by Imaging Proteolytic Activity

Molly R. Darragh[1], Eric L. Schneider[2], Jianlong Lou[4], Paul J. Phojanakong[3], Christopher J. Farady[1], James D. Marks[4], Byron C. Hann[3], and Charles S. Craik[1,2]

Abstract

The cell surface protease membrane-type serine protease-1 (MT-SP1), also known as matriptase, is often upregulated in epithelial cancers. We hypothesized that dysregulation of MT-SP1 with regard to its cognate inhibitor hepatocyte growth factor activator inhibitor-1 (HAI-1), a situation that increases proteolytic activity, might be exploited for imaging purposes to differentiate malignant from normal tissue. In this study, we show that MT-SP1 is active on cancer cells and that its activity may be targeted *in vivo* for tumor detection. A proteolytic activity assay with several MT-SP1–positive human cancer cell lines showed that MT-SP1 antibodies that inhibit recombinant enzyme activity *in vitro* also bind and inhibit the full-length enzyme expressed on cells. In contrast, in the same assay, MT-SP1–negative cancer cell lines were inactive. Fluorescence microscopy confirmed the cell surface localization of labeled antibodies bound to MT-SP1–positive cells. To evaluate *in vivo* targeting capability, 0.7 to 2 nmoles of fluorescently labeled antibodies were administered to mice bearing tumors that were positive or negative for MT-SP1. Antibodies localized to MT-SP1–positive tumors (n = 3), permitting visualization of MT-SP1 activity, whereas MT-SP1–negative tumors (n = 2) were not visualized. Our findings define MT-SP1 activity as a useful biomarker to visualize epithelial cancers using a noninvasive antibody-based method. *Cancer Res; 70(4); 1505–12. ©2010 AACR.*

Introduction

Molecular imaging of cancer has the potential to facilitate early detection and to provide a more detailed assessment of disease. Currently, there are fewer than 10 imaging probes approved for use in the clinic, and they are often limited in use (1). Unfortunately, a lack of specificity and/or sensitivity limits most of these probes for use in evaluating patients with previously diagnosed cancers, and the majority are useful only in a small subset of cancers. Therefore, the search for new biomarker molecules, and for imaging probes with which to detect them, continues.

Proteases are a class of enzymes that shows promise for cancer detection and characterization. Proteolytic processing is necessary in nearly every stage of cancer growth and progression, from angiogenesis to extracellular matrix remodeling, cell-to-cell signaling, and metastasis (2–5). Finely regulated through activation and inhibition, changes in relative levels of proteases or their cognate inhibitors are often associated with cancer, suggesting that it is a dysregulation of proteolysis that contributes to malignant growth (4, 6).

Authors' Affiliations: [1]Graduate Group in Biophysics, [2]Department of Pharmaceutical Chemistry, [3]Helen Diller Family Comprehensive Cancer Center, and [4]Department of Anesthesia, University of California, San Francisco, San Francisco, California

Note: Supplementary data for this article are available at Cancer Research Online (http://cancerres.aacrjournals.org/).

Corresponding Author: Charles S. Craik, Department of Pharmaceutical Chemistry, University of California at San Francisco, 600 16th Street, Mail Code 2280, San Francisco, CA 94158. Phone: 415-476-8146; Fax: 415-502-8298; E-mail: craik@cgl.ucsf.edu.

doi: 10.1158/0008-5472.CAN-09-1640

Membrane-type serine protease 1 (MT-SP1), also referred to as matriptase, prostamin, *TADG-15, PRSS14, SNC19*, and *ST14*, is a cell surface protease that, along with its cognate inhibitor hepatocyte growth factor activator inhibitor-1 (HAI-1), is dysregulated in a number of epithelial cancers. This dysregulation has been correlated to cancer stage, and the downregulation of inhibitors indicates that MT-SP1 is likely more active in the disease state (7–20). MT-SP1 has been shown to cleave a number of cancer-promoting substrates and has recently been associated with a prometastasic signaling pathway in breast cancer; however, its exact role in cancer has not been precisely defined (21–23). The ability to noninvasively monitor active MT-SP1 throughout disease progression would be useful for a better understanding of the role of MT-SP1 in tumor development and as a method for tumor detection.

The use of fluorescently labeled substrate-based probes in mouse models has confirmed that proteolytic activity is a viable marker for cancer imaging *in vivo* (24–27). Antibodies provide an alternate approach for targeting biomarkers and have the advantage of being very potent and specific for the target protease. Pharmacokinetics may also be altered by building the epitope recognition region into antibody-derived structures such as single chain variable fragments (scFv), Fabs, or minibodies. Human antibodies are also nonimmunogenic and can be functionalized for multiple imaging modalities. Accordingly, many antibody-derived tools for cancer detection and treatment are already Food and Drug Administration approved for *in vivo* use (1, 28).

MT-SP1, anchored to the extracellular surface of cancer cells, is localized to malignant tissue and accessible to antibodies, making it an ideal candidate for targeting *in vivo*. Phage display was used to isolate two antibodies that are

selective for the active form of MT-SP1 and to inhibit the protease. Kinetic assays with a number of closely related proteases showed no measurable inhibition, indicating that these antibodies are also very selective for this enzyme (29, 30).[5] Here, we show that MT-SP1 is active and can be inhibited on the surface of human cancer cells. Antibodies are then fluorescently labeled and used as probes for MT-SP1 activity in xenograft mice, ultimately showing that MT-SP1 is active at the tumor site and that this activity may be used for noninvasive tumor detection.

Materials and Methods

Protein Expression and Purification

E2 scFv and Fab and A11 Fab were expressed in *Escherichia coli* and purified as previously described (29, 31). Diabody was synthesized by complete deletion of the polyglycine linker region of the scFv, using the following primers (Eurofins MWG Operon): forward primer 5′-GGCCAAGGCACCCTGGTGACGGTTAGCTCAGCGGATATCGTGATGACCCAGAGC CCACTGAGCCTGCC-3′ and reverse primer 5′-GGCAGGCTCAGTGGGCTCTGGGTCATCAC GATATCCGCTGAGCTAACCGTCACCAGGGTGCCTTGGCC-3′. The scFv expression vector was purified from *E. coli* using Miniprep kit (Qiagen) and subjected to PCR with primers, using reagents from Stratagene QuikChange kit (Agilent Technologies)—1 cycle at 97°C for 60 s, 20 cycles of 97°C for 60 s, 55°C for 80 s, 68°C for 5 min, and 1 cycle of 68°C for 12 min. The PCR product was sequenced to confirm deletion, retransformed into DH12S cells, and expressed in the same way as scFv. The K_I of the diabody was calculated as described below and found to be about twice that of the scFv. MT-SP1 and the inactive zymogen mutant R15A were expressed in *E. coli* and purified as described (29, 31). A11 IgG was expressed in Chinese hamster ovary cells using the V genes from the selected A11 Fab clone and an IgG expression vector as previously described (32).

Kinetics of Inhibition

The K_I for A11 IgG and E2 diabody were determined as previously described (30). The antibody was incubated with recombinant MT-SP1 for 4 h, and proteolysis was measured through activation of the chromogenic substrate Spectrozyme tPA (America Diagnostica, Inc.). A11 concentration was varied from 0 to 250 nmol/L, E2 diabody was varied from 3 to 250 pmol/L, and Spectrozyme concentration was varied from 0 to 1 mmol/L. The K_I^* value for each concentration of substrate was determined by fitting the data to the equation

$$\frac{\nu_i}{\nu_s} = \left\{ \frac{[E_T - I_T - K_I^*] + \sqrt{(I_T + K_I^* - E_T)^2 + (4K_I^* E_T)}}{2E_T} \right\}$$

where υ_i is the reaction velocity in the presence of inhibitor and υ_s is the reaction velocity without inhibitor for a given concentration of substrate. The K_I^* values were then plotted against substrate concentration to obtain the K_I:

$$K_I^* = K_I\left(1 + \frac{[S]}{K_m}\right)$$

Fluorescent Labeling of Protein

scFv, diabody, Fab, and IgG were labeled with AlexaFluor 594 (for microscopy) or AlexaFluor 680 (for *in vivo* imaging; Invitrogen) according to the manufacturer's protocol. Protein was purified from unreacted dye on a Superdex 75 fast protein liquid chromatography column (GE Healthcare). Degree of labeling was determined using UV/Vis spectrometry as directed in the manufacturer's protocol. In fluorescence experiments, concentrations given refer to dye molecules rather than the labeled protein.

Surface Plasmon Resonance

Binding curves were obtained as previously described, with the following modifications: the A11 Fab immobilization level was ~70 RU, and MT-SP1 and the inactive zymogen MT-SP1 R15A was injected in concentrations from 50 nmol/L to 1 μmol/L at 20 μL/min to minimize mass transfer effects (31). Surface regenerations were performed with 100 mmol/L glycine (pH 2.2), allowing a complete return to baseline. The sensorgram of the reference surface was subtracted from the ligand-conjugated surface for each injection.

Cell Culture

Human cancer cell lines HT-29, PC-3, MDA-MB-231, MCF-7, MDA-MB-468, HT1080, and COLO 320DM and LNCaP were obtained from the American Type Culture Collection and maintained in the recommended medium for less than 6 mo after receipt or resuscitation. MCF-7/Luc+ and MDA-MB-231/Luc+ cells were modified by lentiviral transduction to express Firefly luciferase as previously described (33, 34).

Activity assays. T-75 flasks of 70% to 90% confluent adherent cells were rinsed in PBS and lifted using Enzyme-Free Cell Dissociation Buffer (Invitrogen). Cells were washed twice in serum-free medium and counted, then resuspended in serum-free medium and aliquoted into round-bottomed 96-well plates, ranging from 30,000 to 60,000 cells per well, depending on the cell line. E2 Fab and serum-free medium were added for a final volume of 95 μL and final inhibitor concentration of 200 nmol/L. For total inhibition, 5 μL of 25× Complete Inhibitor Cocktail (Roche), a broad-spectrum protease inhibitor cocktail, in water were added along with 90 μL of serum-free medium. After 1- to 1.5-h incubation at 37°C, 5% CO_2, Spectrofluor-tPA (American Diagnostica, Inc.) was added to a final concentration of 500 μmol/L. Fluorescence was measured on a SpectraMax Gemini EM plate reader (MDS, Inc.) with excitation/emission wavelengths of 380/460 nm. Fluorescence was measured for 1 h or until proteolysis ceased to be linear. Fluorescence was also measured

[5] Unpublished results.

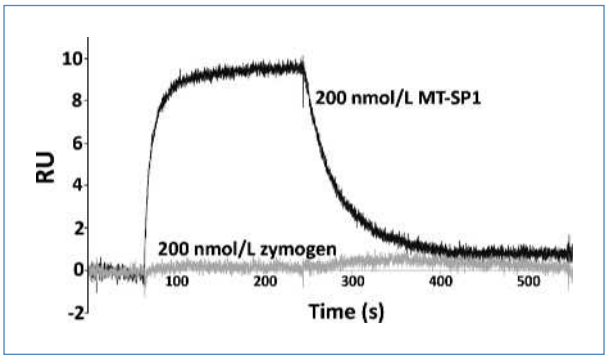

Figure 1. Antibodies are specific for active MT-SP1. SPR binding curves of MT-SP1 (black) and the zymogen-like mutant R15A (gray) to the A11 Fab show robust binding to active enzyme and a lack of binding to the zymogen, indicating that the inhibitor is specific for the active form of the enzyme. Binding assays with enzyme concentrations up to 1 μmol/L showed similar results (not shown). *RU*, resonance unit.

in wells containing only 100 μL of serum-free medium to correct for nonproteolytically mediated substrate hydrolysis. Before inhibition assays, these experiments were carried out with 10,000 to 100,000 cells per well to ensure that the number of cells used was in the range in which fluorescence increased linearly with cell number. Activity assays were conducted in sextuplicate.

Fluorescence imaging. Glass microscope coverslips were flame-sterilized and placed in 12-well plates. Cells were passaged into these wells and grown to a confluency of 40% to 90%. Twelve to 16 h before imaging, cells were switched to serum-free medium. One hour before imaging, fresh serum-free medium was added with enough AlexaFluor 594–labeled E2 scFv to obtain a final fluorphore concentration of 300 nmol/L. Cells were returned to the incubator for 1 to 1.5 h, after which slides were removed, rinsed in PBS, and immediately imaged on a Nikon Eclipse E800 fluorescence microscope outfitted with a G-2E/C filter combination (Nikon). All cells were imaged within 10 min of removal from the incubator. For the HAI-1 blocking experiment, recombinant human HAI-1 (R&D Systems) was diluted to 1 μmol/L in PBS and added along with fresh serum-free medium to a final concentration of 200 nmol/L, and cells were incubated under normal conditions for 3 h. At this time, fluorescently labeled E2 scFv was added to the blocked cells, as well as to unblocked cells, for a final dye concentration of 100 nmol/L. Cells were incubated for another hour and then rinsed in PBS and imaged. Images were collected in the .zvi format with a Zeiss Axiocam using Axiovision Software (Carl Zeiss). Images were converted to jpegs and corrected for camera condensation artifacts, as determined by blank (no cell) images and by using Adobe Photoshop software (Supplementary Data Fig. S1).

Mouse Xenograft Generation

MCF-7 and MCF-7/Luc+ (s.c. implantations). Six- to 7-wk-old female nude (NCR nu/nu athymic female mice, 6–7 wk old; Taconic Farms) were s.c. implanted at the base of tail with 60-d sustained release 0.72 mg 17h-estradiol pellets (Innovative Research of America, Inc.). Two days later, 1×10^7 MCF-7 or MCF-7/Luc+ breast cancer cells were implanted s.c. in the upper back area as a 0.2-mL suspension. Tumor growth was measured by caliper along the largest (length) and smallest (width) axes twice a week. Tumor volumes were calculated using the following formula (20): tumor volume = [(length) × (width) × (width)] / 2. At ~30 d after tumor implantation (mean tumor volume, 600 mm^3), animals were imaged as described below.

MDA-MB-231 (mammary fat pad implantation). Six- to 7-wk-old female nude (NCR nu/nu athymic female mice, 6–7 wk old; Taconic Farms) were anesthetized with avertin. A midline incision along the abdomen followed by angled bilateral incision between the number 4 and 5 nipples was then made to expose the number 4 mammary gland. MDA-MB-231/Luc+ cells (2×10^5 cells suspended in 40 μL serum-free medium) were injected directly into the surgically exposed mammary fat pads with a 500 μL tuberculin syringe. The abdominal skin flaps were closed with wound clips. Wound clips were removed 14 d post-surgery. At ~45 d after tumor implantation (mean tumor volume, 400 mm^3), animals were imaged as described below.

Fluorescence Imaging of Mice

Mice were fed an alfalfa-free diet of Harlan Teklad Global 2018 rodent feed to minimize background fluorescence. Mice were anesthetized with 1.5% to 2% isoflurane. AlexaFluor 680–labeled A11 IgG, E2 Fab, and E2 diabody were injected to the tail veins, with the total amount of injected dye ranging from 0.5 to 2 nmoles. For fluorescence imaging of mice with E2 diabody and Fab, two MCF-7 mice were each injected with ~2 nmoles of dye (Fab) and ~3 nmoles of dye (diabody). Images were collected in fluorescent mode on an IVIS 50 using Living Image 2.50.2 software (Caliper Life Sciences) at set intervals depending on the antibody construct injected. For IgG studies, two MCF-7 and one MCF-7/Luc+ mice were injected with ~2 nmoles of dye and anesthetized and imaged at regular intervals for 50 h. Two MDA-MB-231/Luc+ tumor-bearing mice were injected with ~0.7 to 1 nmoles of dye and imaged in the same manner. All dye was administered in total injection volume equal to 100–300 microliters. In the images presented, region of interest analysis of the entire mouse using Living Image software indicated the relative signal coming from each mouse 4 h after injection. Intensity minima and maxima of each set of the presented images were adjusted to compensate for the difference in total signal from the two sets of mice. For bioluminescent images, Luc+ mice were anesthetized as described and i.v. injected with ~1 mg of luciferase and imaged in bioluminescent mode on the IVIS 50 with Living Image software at 12 to 15 min post-injection. All *in vivo* studies were performed as directed under institutional approval.

Results

Antibodies are selective for active MT-SP1. We have developed two antibodies, E2 and A11, that exclusively bind to the active form of MT-SP1 with picomolar affinity (29, 30). As

Table 1. MT-SP1 inhibition constants of antibody constructs and their applications

Inhibitor	E2		A11	
	scFv	Fab	Fab	IgG
K_I	10 pmol/L	15 pmol/L	720 pmol/L	35 pmol/L
Application	Cell fluorescence	Cell-associated inhibition, *in vivo* imaging	Surface plasmon resonance	*In vivo* imaging

was shown for E2, we show here that the A11 Fab is selective for active MT-SP1 (Fig. 1; ref. 31). Mutating the arginine residue necessary for MT-SP1 autoactivation generates the inactive zymogen MT-SP1 R15A. Whereas binding of active MT-SP1 can be seen at 200 nmol/L, no binding was observed for MT-SP1 R15A at concentrations up to 1 μmol/L, demonstrating selectivity for the active enzyme.

Because they are both selective for active enzyme and share similar mechanisms of inhibition and potencies against MT-SP1, E2 and A11 are used interchangeably in these experiments, as summarized in Table 1. Although multiple antibody-based constructs are used—scFv, Fab, or IgG—they will be referred to throughout as "antibodies," with the specific construct noted in Materials and Methods.

Inhibition of MT-SP1 in cell culture. Although the antibodies inhibit the catalytic domain of MT-SP1, it has not been shown that the full-length enzyme is active and can be inhibited by the antibodies on human cells. An assay was developed to address this by monitoring whole cell–associated proteolysis. In this assay, the P_1-Arg–specific substrate Spectrofluor-tPA was added to cells in serum-free medium, and proteolysis was measured over time. When the MT-SP1–specific (α-MT-SP1) antibodies were added to these cells, any decrease in the rate of proteolysis could be attributed to this particular enzyme, confirming that MT-SP1 is active and that the antibodies inhibit the full-length protease. Figure 2 shows the results of this assay as performed with seven different human cancer cells, chosen based on previously published mRNA expression data (35). The MT-SP1–positive cells showed a 42% to 89% decrease in proteolysis of the P1-Arg substrate on the addition of MT-SP1–specific antibody-based inhibitors, whereas the MT-SP1–negative cells showed no significant decrease in activity. Additionally, the proteolysis was completely inhibited in the presence of a broad spectrum inhibitor cocktail in all cell lines. This assay shows two key points: first, that uninhibited, active MT-SP1 is present on the surface of these cancer cells and, second, that our antibodies are able to bind and inhibit the full-length protease.

Ex vivo *labeling of MT-SP1.* For an antibody to be useful as a probe for molecular imaging of MT-SP1 activity, it must be efficiently labeled without destroying its ability to bind to the enzyme. For fluorescence detection, commercially available dye–succinimidyl ester conjugates were used to nonspecifically label the antibodies through accessible lysines. Based on structural data of both A11 and E2 Fabs bound to recombinant MT-SP1, the labeling of free lysines should not interfere with enzyme binding (Supplementary Data Fig. S2). Depending on the construct—scFv, diabody, Fab, or IgG—we were able to conjugate an average of one to six dye molecules per protein. Inhibition assays with recombinant protein showed minor (0- to 5-fold) increases in IC_{50} values, and given the high potency of these inhibitors, such an increase was not considered a significant barrier to antibody binding. To test the functionality of the scFv against full-length protein, human cancer cells were incubated with the labeled MT-SP1 antibodies and fluorescently imaged to look for association with the membranes of these cells (Fig. 3). Three MT-SP1–positive cell lines—HT-29, MCF-7, and LNCaP—show labeling with the fluorescent antibodies, whereas the negative control lines MDA-MB-231 and COLO 320DM do not. Interesting to note is the difference in the nature of this labeling; the HT-29 signal appears to come evenly from the membrane of the cell whereas the signal on LNCaP and MCF-7 cells is more punctate. Whether this is a result of MT-SP1 congregating on the surface or an internalization of the antibody/enzyme complex has not been determined. Nevertheless, these results show that these labeled antibodies serve as imaging probes to selectively target MT-SP1–positive cells *ex vivo*.

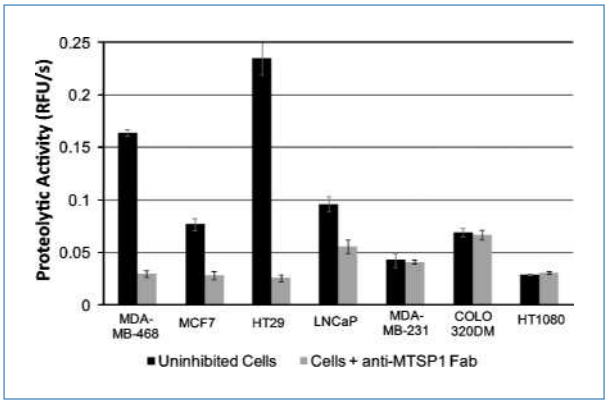

Figure 2. MT-SP1–specific inhibitors reduce cell-associated proteolysis of a fluorescent P1-arginine protease substrate. Spectrofluor-tPA was added to seven human cancer cell lines with and without α-MT-SP1 Fab. Because the inhibitors are specific, any reduction in proteolysis can be attributed to an inhibition of active MT-SP1. Black bars represent total P_1-Arg proteolytic activity of uninhibited cells, whereas gray bars show the activity of cells incubated with α-MT-SP1 Fab. Cell lines that express MT-SP1 mRNA—MDA-MB-468, MCF-7, HT29, and LNCaP—show a reduction in proteolysis on the addition of antibody inhibitor, whereas the MT-SP1–negative cell lines MDA-MB-231, HT1080, and COLO 320DM do not. *RFU*, relative fluorescence units.

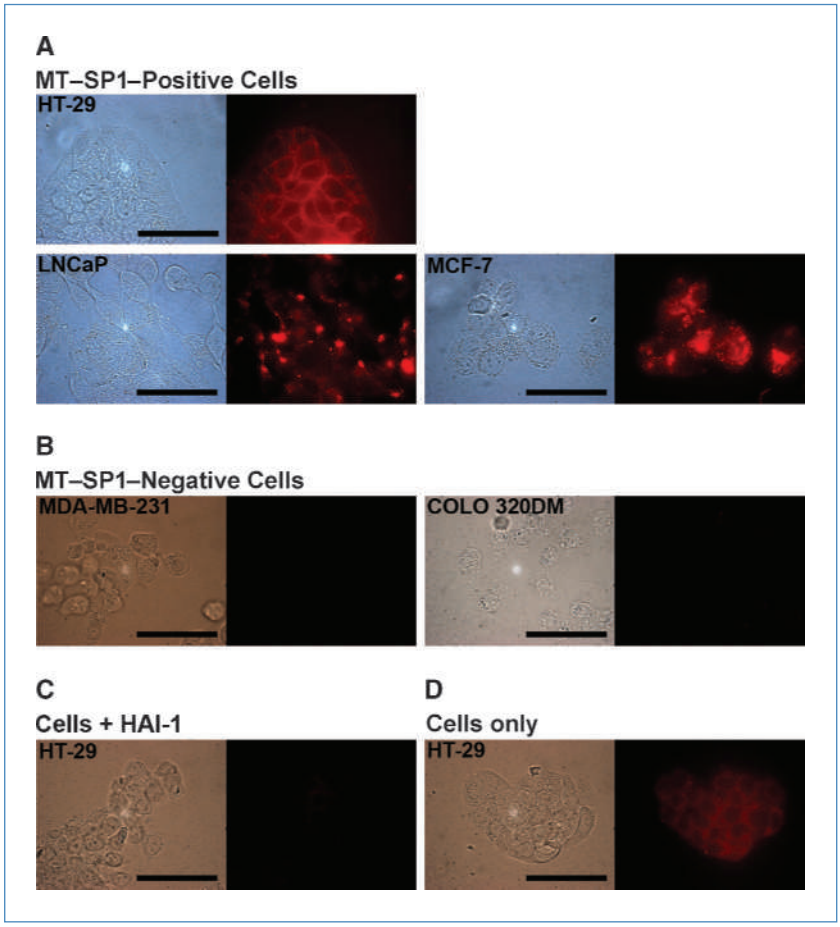

Figure 3. Fluorescently labeled α-MT-SP1 scFv localizes to MT-SP1–positive cells in cell culture. A, HT-29, LNCaP, and MCF-7 cells express MT-SP1 mRNA, whereas MDA-MD-231 and COLO 320DM cells (B) do not. Antibodies do not significantly displace HAI-1. HT-29 cells that have been incubated with recombinant HAI-1 (C) show much less surface labeling on exposure to fluorescently labeled scFv than those that have not been blocked (D). Scale bar, 50 μm. Images were corrected as described in Supplementary materials.

MT-SP1 is putatively present on the surface of epithelial cells in at least three different forms—the inactive zymogen, active protease, and HAI-1–inhibited protease. Our experimental results indicate that the antibodies are binding to and inhibiting active protease on the cell surface; however, the question remains whether the antibody is displacing cognate inhibitor on binding. In this case, the signal would not be representative of free, active protease on the cell surface. A study of the rat homologues of MT-SP1 and HAI-1 observed picomolar inhibition, and MT-SP1, which has been shed from the cell surface, is found only in complex with its cognate inhibitor, suggesting extremely tight binding *in vivo* (36). To test for HAI-1 displacement by these antibodies, the immunofluorescence cell labeling was carried out with HT-29 cells, which were first incubated with recombinant HAI-1 (Fig. 3C and D). Cells that were treated with HAI-1 before the addition of fluorescently labeled scFv showed much lower membrane-associated fluorescence than those that were not treated. These data show that our antibodies only minimally displace HAI-1 under the conditions used in the fluorescence and the cell activity experiments, indicating that the majority of the signal comes from free active MT-SP1.

***Targeting MT-SP1* in vivo.** Having successfully labeled active MT-SP1 in cell culture, the antibodies were evaluated as probes for MT-SP1 activity *in vivo*. Based on cell culture data, xenograft mouse models were generated using MCF-7, MCF-7/Luc+, and MDA-MB-231/Luc+ breast cancer cell lines. The "Luc+" designation indicates that the cells have been transfected with an imaging vector that includes the gene for Firefly luciferase so that the tumor can be imaged through bioluminescence detection independent of MT-SP1–based fluorescence detection (34). These mouse models were injected with fluorescently labeled diabody, Fab, or IgG, and imaged for up to 50 hours to assess biodistribution of antibodies and any tumor localization. The anti–MT-SP1 diabody and Fab localized to the tumor in MCF-7 xenograft mice but failed to achieve high tumor/background contrast due to high levels of signal retained in the excretory system (Supplementary Data Fig. S3). The IgG, however, localized to the tumor in both MCF-7 and MCF-7/Luc+ mice and remained so until free protein was cleared, achieving excellent tumor to background contrast by 50 hours (Fig. 4A; Supplementary Data Fig. S4). Similar injections into MDA-MB-231/Luc+ tumor-bearing mice showed no tumor-associated signal over the same period (Fig. 4B). Luciferin administered to these mice generated a tumor-specific signal, validating both the presence of the MCF-7/Luc+ and MDA-MB-231/Luc+ cells at this location and sufficient vasculature to deliver the

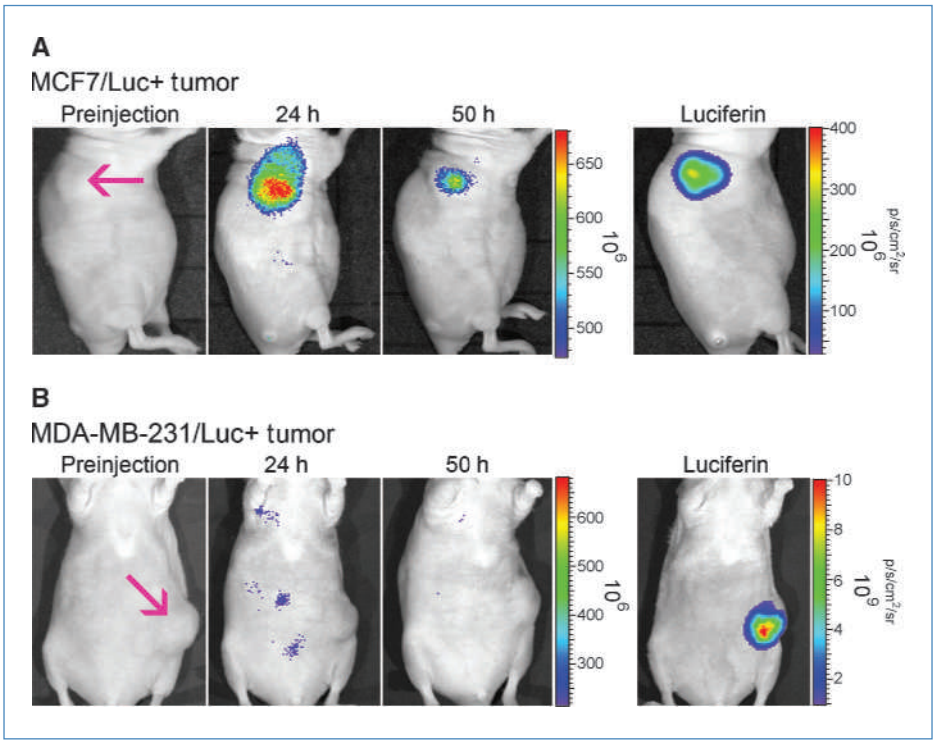

Figure 4. α-MT-SP1 antibodies are able to selectively target MT-SP1–positive tumors *in vivo*. AlexaFluor 680–labeled A11 IgG was injected and imaged using a two-dimensional fluorescence imager. Tumors are indicated by arrows. In MCF-7/Luc+ xenograft mice, the tumors become selectively labeled with minimal background after 50 h (A). In the MDA-MB-231/Luc+ (MT-SP1–negative) models, however, no tumor labeling was seen over the same period (B). As an alternate method for detecting the tumors, mice were injected with ~2 mg of luciferin and imaged after 10 to 15 min. Because the Luc+ cells have been engineered to express luciferase, a bioluminescent signal is seen at the tumor, confirming location and viability of the xenograft.

labeled antibodies to the tumor. These experiments indicate that MT-SP1 is active in the tumors that are positive for MT-SP1 expression, and that this activity can be targeted *in vivo* for noninvasive cancer imaging using the antibodies as probes.

Discussion

Proteases have long been recognized as cancer biomarkers; however, based on indications that it is activity that is important for cancer progression, perhaps a more direct strategy for disease assessment is to measure the active form of the enzyme. The approach described here, from phage display to *in vivo* imaging, could be readily applied to any number of cancer-associated proteases, particularly those anchored to the cell membrane, to identify additional sites for targeting tumors *in vivo*.

The tools described here may have many uses in studying MT-SP1 both in the laboratory and the clinic. Although immunohistochemistry and expression data have strongly connected MT-SP1 to cancer, these experiments have focused on overall protein levels rather than the amount of proteolytic activity. The antibody-mediated targeting of active MT-SP1 described here may provide a new way to measure protease activity and connect it with specific downstream effects both in cell culture and in mouse models, such as the recently proposed prometastatic signaling pathway involving MT-SP1, the growth factor MSP, and its receptor RON (22, 23).

These antibodies may also prove useful for studying the biology of MT-SP1 at the cellular level. Recent results have shown that HAI-1 recycles between the membranes of polarized epithelial cells, and it is proposed that MT-SP1 may be transported between membranes in a similar fashion, perhaps in complex with HAI-1 (37). Although further studies are necessary, it is possible that the punctuate fluorescence observed when the labeled antibodies are added to unfixed MCF7 and LNCaP cells is a result of internalization of antibody-bound enzyme, indicating that MT-SP1 is indeed capable of reentering the cell after it is exocytosed to the extracellular membrane.

MT-SP1 detection and inhibition may also find use in the clinic. Small-molecule inhibitors of MT-SP1 have shown that *in vivo* inhibition has potential in anticancer therapy (38). Antibodies could achieve similar results while allowing for more specific targeting and inhibition, minimizing toxicity. As an imaging biomarker, MT-SP1 expression has been correlated with cancer stage and/or subtype, and a noninvasive method for assessing the activity in the malignant tissue may aid in tumor classification and potential therapeutic design. Independent of the utility of MT-SP1 inhibition in cancer therapy, it can be used as an imaging biomarker to assess tumor margin or monitor tumor response to alternative therapies in MT-SP1–positive tumors.

Previous studies connecting MT-SP1 and related type 2 transmembrane serine proteases to cancer have suggested their potential as biomarkers (39). This work shows that MT-SP1 activity is present in tumors and can be targeted and inhibited on the surface of cancer cells using specific antibodies, validating an approach that can be used to target cell surface proteolysis for cancer assessment and intervention.

Disclosure of Potential Conflicts of Interest

The authors declare no competing commercial interest with the work presented here.

Acknowledgments

We thank Lily Darragh for technical consultation and Dr. Mark Moasser for useful discussions and critical reading of the manuscript.

Grant Support

National Science Foundation Graduate Research Fellowship, Chih Family Foundation Award, and ARCS Foundation Scholarship (M.R. Darragh), Department of Defense Breast Cancer Research Program BC043431 (C.J. Farady), and NIH grants CA72006 and CA128765 (C.S. Craik) and CA108462-04 (E.L. Schneider).

The costs of publication of this article were defrayed in part by the payment of page charges. This article must therefore be hereby marked *advertisement* in accordance with 18 U.S.C. Section 1734 solely to indicate this fact.

Received 5/8/09; revised 12/1/09; accepted 12/3/09; published OnlineFirst 2/9/10.

References

1. Kelloff GJ, Krohn KA, Larson SM, et al. The progress and promise of molecular imaging probes in oncologic drug development. Clin Cancer Res 2005;11:7967–85.
2. Mignatti P, Rifkin DB. Biology and biochemistry of proteinases in tumor invasion. Physiol Rev 1993;73:161–95.
3. Andreasen PA, Egelund R, Petersen HH. The plasminogen activation system in tumor growth, invasion, and metastasis. Cell Mol Life Sci 2000;57:25–40.
4. Egeblad M, Werb Z. New functions for the matrix metalloproteinases in cancer progression. Nat Rev Cancer 2002;2:161–74.
5. Jedeszko C, Sloane BF. Cysteine cathepsins in human cancer. Biol Chem 2004;385:1017–27.
6. Parr C, Watkins G, Mansel RE, Jiang WG. The hepatocyte growth factor regulatory factors in human breast cancer. Clin Cancer Res 2004;10:202–11.
7. Takeuchi T, Shuman MA, Craik CS. Reverse biochemistry: use of macromolecular protease inhibitors to dissect complex biological processes and identify a membrane-type serine protease in epithelial cancer and normal tissue. Proc Natl Acad Sci U S A 1999;96:11054–61.
8. Lin CY, Wang JK, Torri J, Dou L, Sang QA, Dickson RB. Characterization of a novel, membrane-bound, 80-kDa matrix-degrading protease from human breast cancer cells. Monoclonal antibody production, isolation, and localization. J Biol Chem 1997;272:9147–52.
9. Shi YE, Torri J, Yieh L, Wellstein A, Lippman ME, Dickson RB. Identification and characterization of a novel matrix-degrading protease from hormone-dependent human breast cancer cells. Cancer Res 1993;53:1409–15.
10. Lin CY, Anders J, Johnson M, Sang QA, Dickson RB. Molecular cloning of cDNA for matriptase, a matrix-degrading serine protease with trypsin-like activity. J Biol Chem 1999;274:18231–6.
11. Jin JS, Chen A, Hsieh DS, Yao CW, Cheng MF, Lin YF. Expression of serine protease matriptase in renal cell carcinoma: correlation of tissue microarray immunohistochemical expression analysis results with clinicopathological parameters. Int J Surg Pathol 2006;14:65–72.
12. Jin JS, Hsieh DS, Loh SH, Chen A, Yao CW, Yen CY. Increasing expression of serine protease matriptase in ovarian tumors: tissue microarray analysis of immunostaining score with clinicopathological parameters. Mod Pathol 2006;19:447–52.
13. Tsai WC, Chu CH, Yu CP, et al. Matriptase and survivin expression associated with tumor progression and malignant potential in breast cancer of Chinese women: tissue microarray analysis of immunostaining scores with clinicopathological parameters. Dis Markers 2008;24:89–99.
14. Santin AD, Zhan F, Bignotti E, et al. Gene expression profiles of primary HPV16- and HPV18-infected early stage cervical cancers and normal cervical epithelium: identification of novel candidate molecular markers for cervical cancer diagnosis and therapy. Virology 2005;331:269–91.
15. Riddick AC, Shukla CJ, Pennington CJ, et al. Identification of degradome components associated with prostate cancer progression by expression analysis of human prostatic tissues. Br J Cancer 2005;92:2171–80.
16. Cheng MF, Tzao C, Tsai WC, et al. Expression of EMMPRIN and matriptase in esophageal squamous cell carcinoma: correlation with clinicopathological parameters. Dis Esophagus 2006;19:482–6.
17. Hoang CD, D'Cunha J, Kratzke MG, et al. Gene expression profiling identifies matriptase overexpression in malignant mesothelioma. Chest 2004;125:1843–52.
18. Saleem M, Adhami VM, Zhong W, et al. A novel biomarker for staging human prostate adenocarcinoma: overexpression of matriptase with concomitant loss of its inhibitor, hepatocyte growth factor activator inhibitor-1. Cancer Epidemiol Biomarkers Prev 2006;15:217–27.
19. Oberst MD, Johnson MD, Dickson RB, et al. Expression of the serine protease matriptase and its inhibitor HAI-1 in epithelial ovarian cancer: correlation with clinical outcome and tumor clinicopathological parameters. Clin Cancer Res 2002;8:1101–7.
20. Tsai WC, Sheu LF, Chao YC, Chen A, Chiang H, Jin JS. Decreased matriptase/HAI-1 ratio in advanced colorectal adenocarcinoma of Chinese patients. Chin J Physiol 2007;50:225–31.
21. Darragh MR, Bhatt AS, Craik CS. MT-SP1 proteolysis and regulation of cell-microenvironment interactions. Front Biosci 2008;13:528–39.
22. Bhatt AS, Welm A, Farady CJ, Vasquez M, Wilson K, Craik CS. Coordinate expression and functional profiling identify an extracellular proteolytic signaling pathway. Proc Natl Acad Sci U S A 2007;104:5771–6.
23. Welm AL, Sneddon JB, Taylor C, et al. The macrophage-stimulating protein pathway promotes metastasis in a mouse model for breast cancer and predicts poor prognosis in humans. Proc Natl Acad Sci U S A 2007;104:7570–5.
24. Weissleder R, Tung CH, Mahmood U, Bogdanov A, Jr. *In vivo* imaging of tumors with protease-activated near-infrared fluorescent probes. Nat Biotechnol 1999;17:375–8.
25. Blum G, von Degenfeld G, Merchant MJ, Blau HM, Bogyo M. Noninvasive optical imaging of cysteine protease activity using fluorescently quenched activity-based probes. Nat Chem Biol 2007;3:668–77.
26. Joyce JA, Baruch A, Chehade K, et al. Cathepsin cysteine proteases are effectors of invasive growth and angiogenesis during multistage tumorigenesis. Cancer Cell 2004;5:443–53.
27. Jiang T, Olson ES, Nguyen QT, Roy M, Jennings PA, Tsien RY. Tumor imaging by means of proteolytic activation of cell-penetrating peptides. Proc Natl Acad Sci U S A 2004;101:17867–72.
28. Wu AM, Senter PD. Arming antibodies: prospects and challenges for immunoconjugates. Nat Biotechnol 2005;23:1137–46.
29. Sun J, Pons J, Craik CS. Potent and selective inhibition of membrane-type serine protease 1 by human single-chain antibodies. Biochemistry 2003;42:892–900.
30. Farady CJ, Sun J, Darragh MR, Miller SM, Craik CS. The mechanism of inhibition of antibody-based inhibitors of membrane-type serine protease 1 (MT-SP1). J Mol Biol 2007;369:1041–51.
31. Farady CJ, Egea PF, Schneider EL, Darragh MR, Craik CS. Structure of an Fab-protease complex reveals a highly specific non-canonical mechanism of inhibition. J Mol Biol 2008;380:351–60.
32. Nowakowski A, Wang C, Powers DB, et al. Potent neutralization of botulinum neurotoxin by recombinant oligoclonal antibody. Proc Natl Acad Sci U S A 2002;99:11346–50.

33. Ray P, De A, Min JJ, Tsien RY, Gambhir SS. Imaging tri-fusion multimodality reporter gene expression in living subjects. Cancer Res 2004;64:1323–30.

34. Ray P, Gambhir SS. Noninvasive imaging of molecular events with bioluminescent reporter genes in living subjects. Methods Mol Biol 2007;411:131–44.

35. Bhatt AS, Takeuchi T, Ylstra B, et al. Quantitation of membrane type serine protease 1 (MT-SP1) in transformed and normal cells. Biol Chem 2003;384:257–66.

36. Kojima K, Tsuzuki S, Fushiki T, Inouye K. Roles of functional and structural domains of hepatocyte growth factor activator inhibitor type 1 in the inhibition of matriptase. J Biol Chem 2008;283:2478–87.

37. Godiksen S, Selzer-Plon J, Pedersen ED, et al. Hepatocyte growth factor activator inhibitor-1 has a complex subcellular itinerary. Biochem J 2008;413:251–9.

38. Uhland K. Matriptase and its putative role in cancer. Cell Mol Life Sci 2006;63:2968–78.

39. Bugge TH, Antalis TM, Wu Q. Type II transmembrane serine proteases. J Biol Chem 2009;284:23177–81.